



泛在计算与智能系统研究中心
Research Center of Ubiquitous Computing and Intelligent Systems



哈爾濱工業大學
Harbin Institute of Technology

Large-Scale Multi-Robot Coverage Path Planning via Local Search

Jingtao Tang, Hang Ma

Simon Fraser University

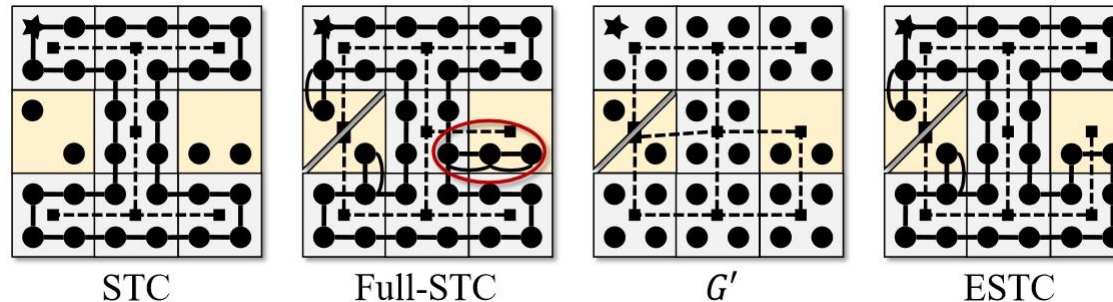
AAAI 2024

Chenxin Cai
Oct. 8th, 2024

Motivation-1

“Large-Scale Multi-Robot Coverage Path Planning via Local Search”. AAAI, 2024.

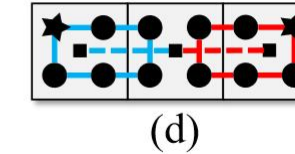
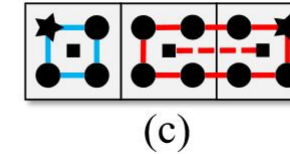
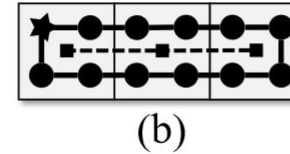
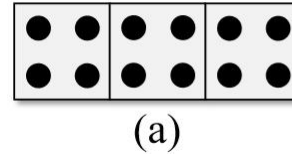
- Graph-based 方法只处理地图上能够完整划分成 2×2 的部分
- Full-STC 存在次优 (suboptimal) 的情况 → 提出 Extended-STC



Motivation-2

“Large-Scale Multi-Robot Coverage Path Planning via Local Search”. AAAI, 2024.

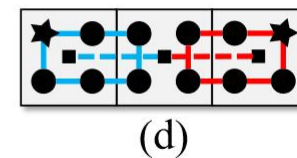
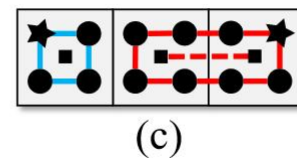
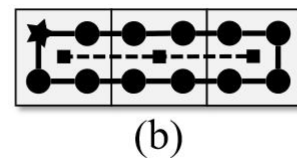
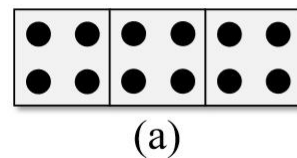
- Graph-based 方法存在suboptimal情况 → 提出 LS-MCPP



Problem Formulation

“Large-Scale Multi-Robot Coverage Path Planning via Local Search”. AAAI, 2024.

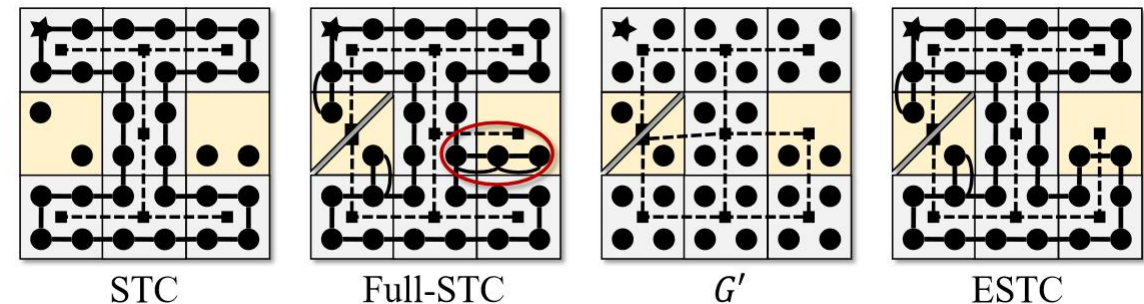
- 2D grid terrain graph $G = (V_g, E_g)$
- decomposed graph $D = (V_d, E_d)$
- $\delta_v \in V_g, v \in V_d$
- $\varepsilon = (\delta_u, \delta_v) \in E_g$



Full-STC v.s. Extended-STC

“Large-Scale Multi-Robot Coverage Path Planning via Local Search”. AAAI, 2024.

- G' : 去掉 G 的一些边
- 斜对角的情况，拆分成两个点



- 赋予边 $\varepsilon = (\delta_u, \delta_v)$ 权重

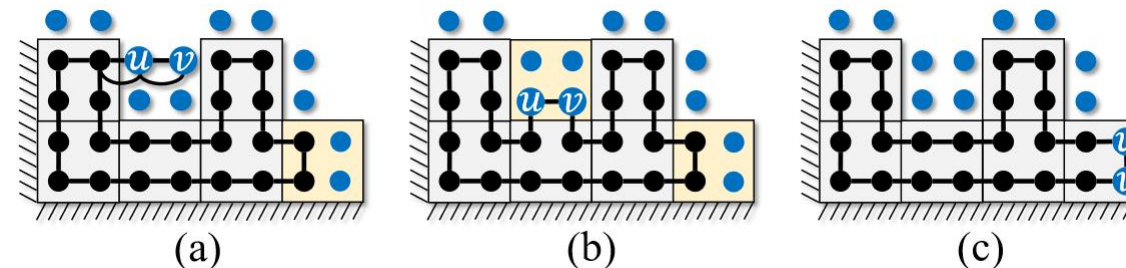
$$w_{\max} \cdot \frac{1}{2} \cdot \left(\sum_{\varepsilon \sim \delta_u} w_\varepsilon + \sum_{\varepsilon \sim \delta_v} w_\varepsilon \right) \quad (1)$$

where w_{\max} is the maximal edge weights of E_g to prioritize using edges connecting complete terrain vertices. Fig. 2

Grow Operators

“Large-Scale Multi-Robot Coverage Path Planning via Local Search”. AAAI, 2024.

- $V^+ = \{v \in V_d | n_v > 1\}$ 表示被多次覆盖的点集合, n_v 记录 v 在 subgraph 中被覆盖的次数
- $o_g(i, e)$
- $e = (u, v)$ 是有效的 当且仅当 D_i 存在与之平行的边 (p, q)
- 执行完 $o_g(i, e)$, 如果 $e = (u, v)$ 被其他 subgraph 覆盖, 则将 u, v 加入 V^+



Deduplicate Operators

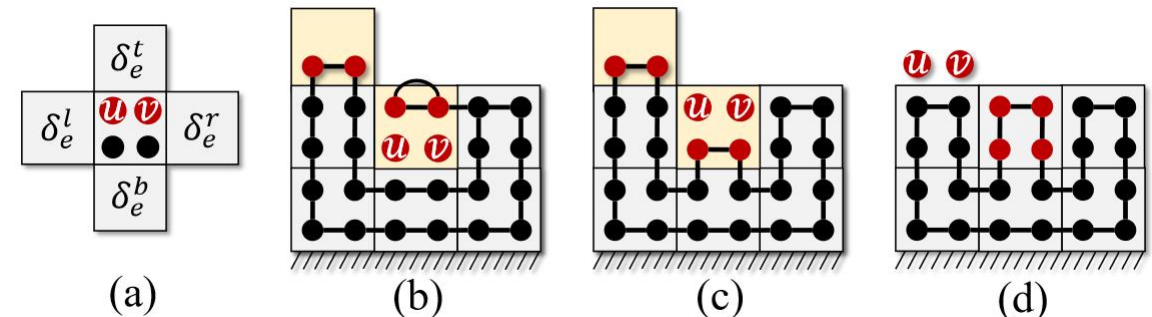
“Large-Scale Multi-Robot Coverage Path Planning via Local Search”. AAAI, 2024.

- $o_d(i, e)$
- 判定 $e = (u, v)$ 是有效的（可以被移除的） $\rightarrow u, v \in V^+ \cap V_{d,i}$

且移除 e 之后 D_i 仍然是连通的

- δ_u 是 complete 的
 - δ_e^t 不在 $V_{g,i}$ 中
 - δ_e^b 中所有的点都在 $V_{g,i}$ 中

- 如果 $\delta = \delta_e^l, \delta_e^r$ 在 $V_{g,i}$ 中，那么 δ 中所有的点、 δ 与 δ_e^b 相邻的点都要在 $V_{g,i}$ 中



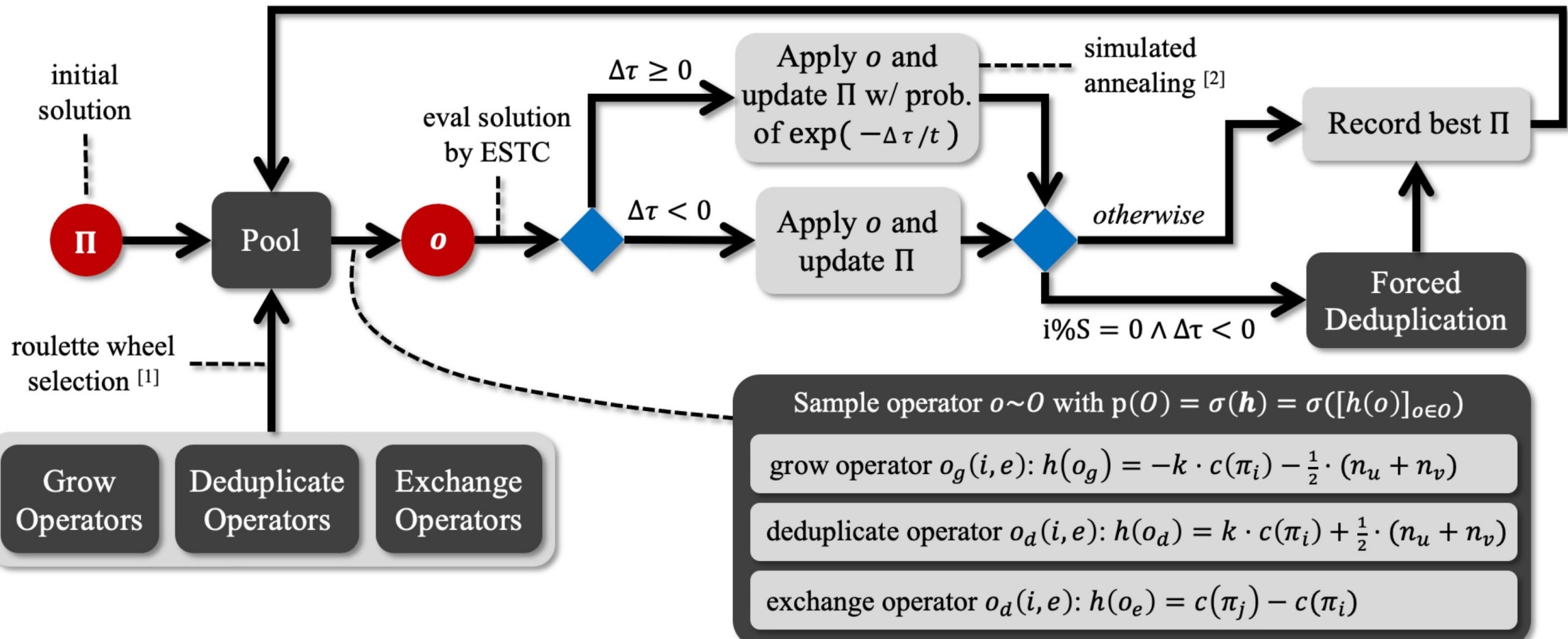
Exchange Operators

“Large-Scale Multi-Robot Coverage Path Planning via Local Search”. AAAI, 2024.

- $o_e(i, j, e)$ 表示 $o_g(i, e)$ 和 $o_d(j, e)$, D_i 增加边 $e = (u, v)$, D_i 删除边 $e = (u, v)$

Framework

“Large-Scale Multi-Robot Coverage Path Planning via Local Search”. AAAI, 2024.



Forced Deduplication

“Large-Scale Multi-Robot Coverage Path Planning via Local Search”. AAAI, 2024.

- 消除U-turn

```
20 Function FORCEDDEDUPLICATION( $\Pi, O_d$ ):  
21   for  $i \in \arg \text{sort}(\{c(\pi_i)\}_{i \in I})$  do  
22     while  $(u, v) \leftarrow$  any U-turn in  $\pi_i$  do  
23       Remove  $u, v$  from  $D_i$  and update  $\pi_i$   
24   for  $i \in \arg \text{sort}(\{c(\pi_i)\}_{i \in I})$  do  
25     while  $\{o_d(j, e) \in O_d \mid i = j\} \neq \emptyset$  do  
26        $o \leftarrow \arg \min \left( [h(o)]^T_{o \in \{o_d(j, e) \in O_d \mid i = j\}} \right)$   
27       Apply operator  $o$ , update  $\Pi$  and  $O_d$ 
```

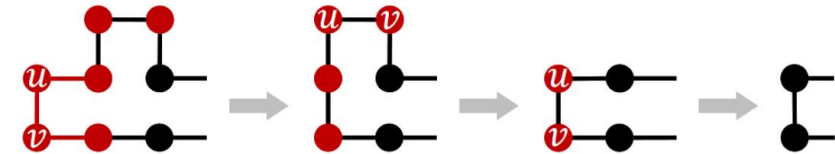
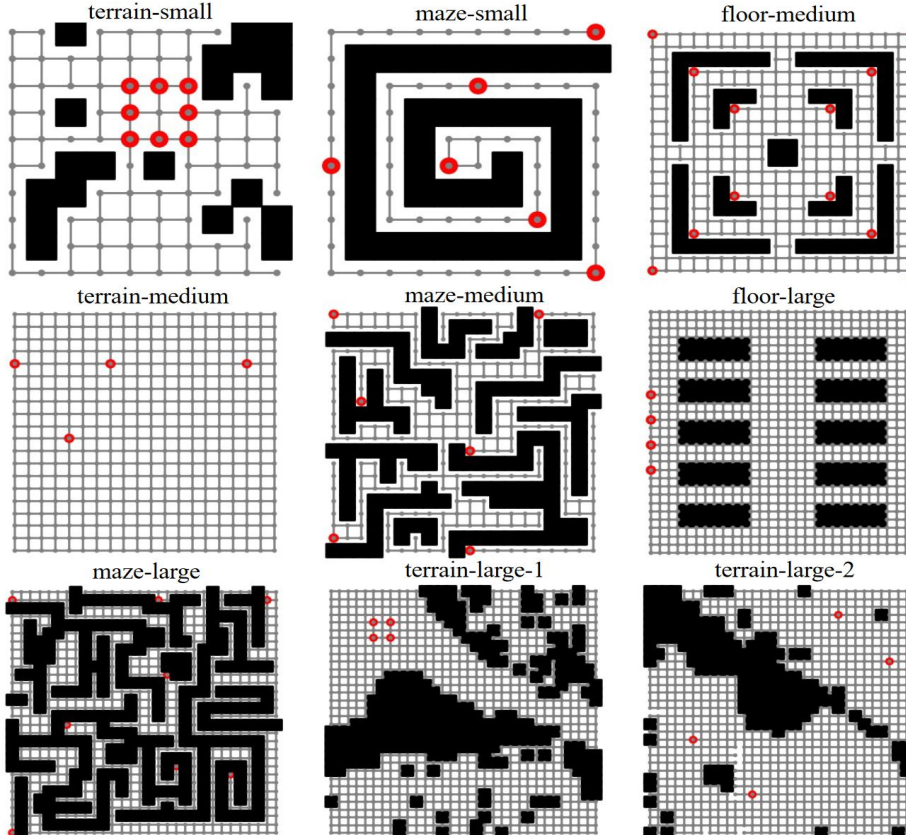


Figure 5: FORCEDDEDUPLICATION() executed on a coverage path π_i . Each red circle represents a duplication of $V_{d,i}$. In each frame, a U-turn $(u, v) \in \pi_i$ is found and u, v are removed from π_i until no U-turn exists.

Experiments

Instances

“Mixed Integer Programming for Time-Optimal Multi-Robot Coverage Path Planning with Efficient Heuristics”. RA-L, 2023.



Instance	Grid spec.	% of obs.	V	E	k	# of vars.	weighted
<i>floor-small</i>	5×10	8.0%	46	73	4	1061	✗
<i>terrain-small</i>	10×10	20.0%	80	121	8	3545	✓
<i>maze-small</i>	10×10	40.0%	60	60	6	1441	✗
<i>floor-medium</i>	20×20	19.0%	324	524	12	22753	✗
<i>terrain-medium</i>	20×20	0.0%	400	760	4	10721	✓
<i>maze-medium</i>	20×20	39.0%	244	303	6	6919	✗
<i>floor-large</i>	30×30	15.56%	760	1370	4	19481	✗
<i>maze-large</i>	30×30	38.56%	553	717	8	21633	✗
<i>terrain-large-1</i>	32×32	27.83%	739	1275	4	18257	✓
<i>terrain-large-2</i>	32×32	19.53%	824	1495	4	21237	✓

Fig. 5: MMRCT instances for MCPP performance evaluation.

Instances

“Large-Scale Multi-Robot Coverage Path Planning via Local Search”. AAAI, 2024.

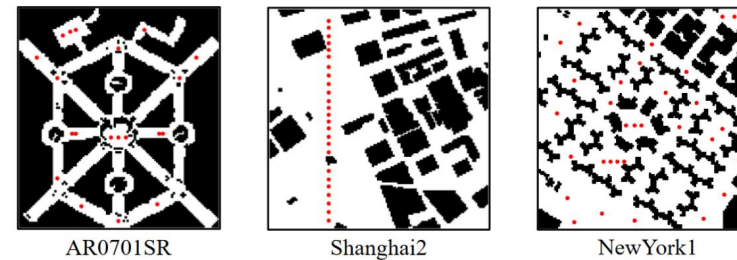


Figure 6: Three very large-scale MCPP instances adopted from 2D pathfinding benchmarks (Sturtevant 2012). Red circles represent the initial vertices of robots.

Instance	Grid spec.	$ V_g $	$ E_g $	k	weighted
<i>AR0701SR</i>	107×117	4,860	8,581	20	✓
<i>Shanghai2</i>	128×128	11,793	22,311	25	✗
<i>NewYork1</i>	128×128	11,892	21,954	32	✓

Ablation Study

“Large-Scale Multi-Robot Coverage Path Planning via Local Search”. AAAI, 2024.

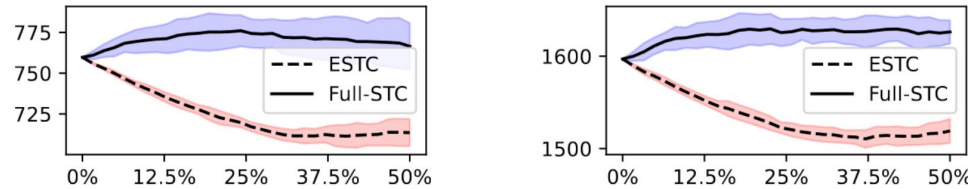


Figure 7: Single-robot coverage path costs (y-axis) with the percentages of incomplete terrain vertices (x-axis). Left and right sub-figures correspond to *flr-l* and *trn1-l*, respectively.

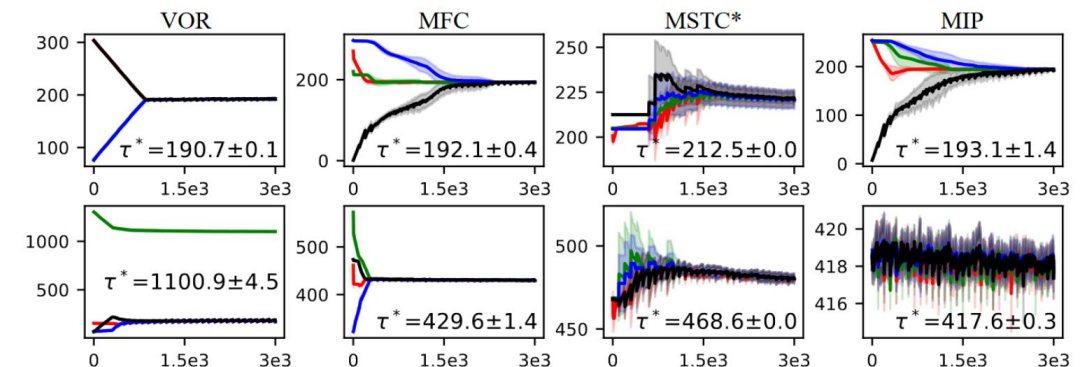


Figure 8: Path costs (y-axis) of 4 robots for LS-MCPP over iterations (x-axis) with different initial solutions. The upper and lower rows correspond to *flr-l* and *trn1-l*, respectively.

Ablation Study

“Large-Scale Multi-Robot Coverage Path Planning via Local Search”. AAAI, 2024.

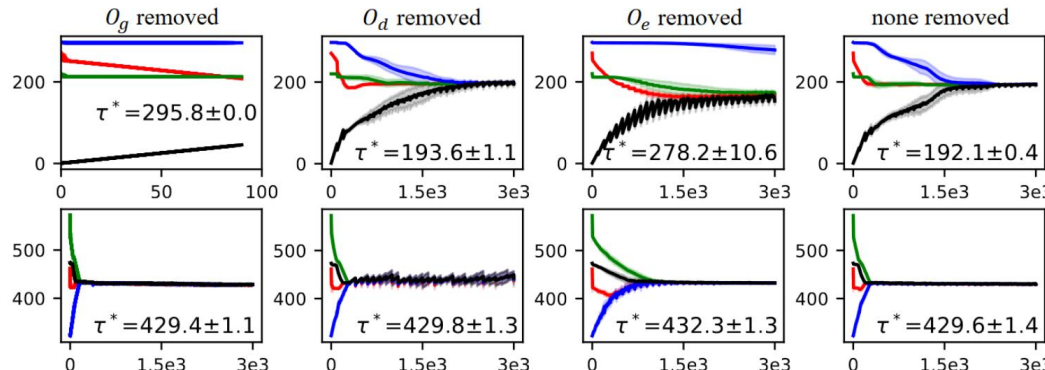


Figure 9: Path costs (y-axis) of 4 robots for LS-MCPP over iterations (x-axis) with different operators removed. The upper and lower row correspond to *flr-l* and *trn1-l*, respectively.

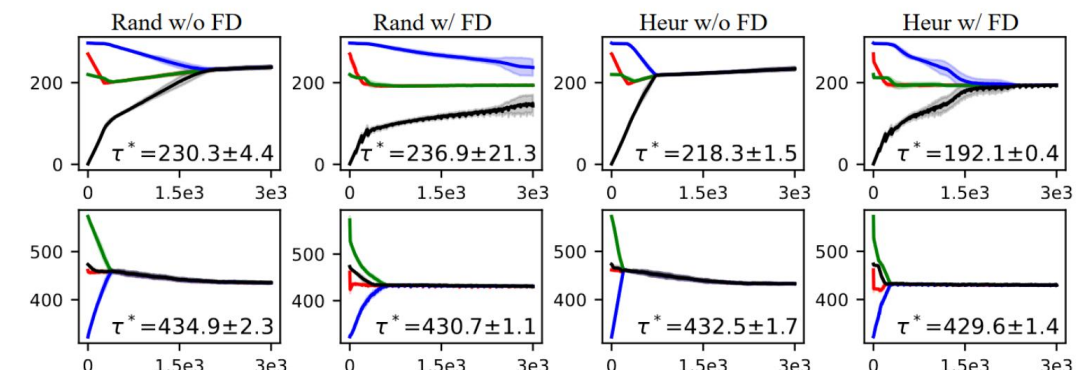


Figure 10: Path costs (y-axis) of 4 robots for LS-MCPP over iterations (x-axis) with different operator sampling and whether FORCEDDEDUPLICATION (FD) is used. The upper and lower row correspond to *flr-l* and *trn1-l*, respectively.

Comparative Study

“Large-Scale Multi-Robot Coverage Path Planning via Local Search”. AAAI, 2024.

	VOR	MFC	MSTC*	MIP(H)	MIP		LS-MCPP (Ours)		
<i>flr-s</i>	42.75	23	21	16	0.0%	16	0.0%	16.75 ± 0.3	21.5 ± 2.1
	0.01s	0.03s	0.02s	13s	%	20s	%	5.3 ± 0.13 s	3.6 ± 2.9 s
<i>trn-m</i>	420.2	368.2	269.5	246.7	0.6%	246.7	1.6%	244.5 ± 0.8	245 ± 12.2
	0.04s	0.58s	0.32s	24h	%	24h	%	17.8 ± 0.1 s	19.6 ± 1.3 s
<i>mze-m</i>	134.8	67	69	52	0.0%	51	20%	54.3 ± 2.9	65.0 ± 4.2
	0.02s	0.35s	0.34s	4.9s	%	24h	%	10.7 ± 0.1 s	9.0 ± 2.9 s
<i>flr-l</i>	303.8	294	212.5	207	8.3%	254	25%	192.1 ± 0.4	207 ± 20.2
	0.07s	2.37s	0.09s	24h	%	24h	%	30.5 ± 1.3 s	35.2 ± 1.6 s
<i>mze-l</i>	193.8	105	139.5	91.5	0.0%	93	25%	97.3 ± 0.5	104.8 ± 7.6
	0.04s	0.10s	0.58s	54s	%	24h	%	15.4 ± 0.2 s	12.9 ± 5.8 s
<i>trn1-l</i>	1,303	597.4	468.6	435.1	9.7%	419.1	6.1%	429.6 ± 1.4	444 ± 11.2
	0.07s	1.67s	1.93s	24h	%	24h	%	34.3 ± 0.4 s	37.3 ± 1.6 s
<i>AR07</i>	1,301	1,254	878.7	1,351	42%	1,333	55%	805.9 ± 7.9	$1,024 \pm 74$
	0.47s	36.9s	9.91s	24h	%	24h	%	6.3 ± 0.1 m	6.2 ± 0.3 m
<i>Shanghai2</i>	1,451	754	576.5	1,509	59%	/	/	570.9 ± 2.1	719 ± 73.0
	1.21s	7.2m	2.21s	24h	%	/	/	17.6 ± 2.1 m	12.5 ± 0.8 m
<i>New York1</i>	1,735	1,530	1,208	4,736	80%	/	/	$1,062 \pm 14$	$1,563 \pm 110$
	1.13s	2.4m	20.2s	24h	%	/	/	15.0 ± 4.1 m	12.6 ± 0.5 m